Assessing Changes in US Regional Precipitation on Multiple Time Scales

Ross McKitrick
Department of Economics and Finance
University of Guelph
Guelph ON Canada N1G 2W1
ross.mckitrick@uoguelph.ca

John Christy
Earth System Science Center
University of Alabama in Huntsville

Journal of Hydrology 2019 https://doi.org/10.1016/j.jhydrol.2019.124074

Keywords: US Regional Precipitation; Long Term Persistence; Time Scales; Twentieth Century; Extreme Events.

This research did not receive any specific grant from funding agencies in the public, commercial, or not-for-profit sectors.

Data Statement: All data and R code will be posted online with the published article.

Abstract: We estimate trends in US regional precipitation on multiple time spans and scales relevant to the detection of changes in climatic regimes. A large literature has shown that trend estimation in hydrological series may be affected by long-term persistence (LTP) and selection of sample length. We show that 2,000-year proxy-based reconstructions of the Palmer Modified Drought Index for the US Southeast (SE) and Pacific Coast (PC) regions exhibit LTP and reveal post-1900 changes to be within the range of longer-term natural fluctuations. We also use a new data base of daily precipitation records for 20 locations (10 PC and 10 SE) extending back in many cases to the 1870s. Over the 1901-2017 interval upward trends in some measures of average and extreme precipitation appear, but they are not consistently significant and in the full records back to 1872 they largely disappear. They also disappear or reverse in the post-1978 portion of the data set, which is inconsistent with them being responses to enhanced greenhouse gas forcing. We conclude that natural variability is likely the dominant driver of historical changes in precipitation and hence drought dynamics in the US SE and PC.

1 INTRODUCTION

Understanding the full range of historical precipitation patterns is essential for detecting whether long term averages and extremes have changed and whether anthropogenic forcing is likely to dominate future trends. The recent US Climate Science Special Report (USGCRP 2017) concluded that United States average precipitation increased by 4% over 1901-2016, largely due to increases in the fall season (p. 207), and that heavy precipitation events throughout most of the US increased in both intensity and frequency. It also concludes "confidence is *high* that precipitation extremes will increase in frequency and intensity in the future" throughout the US (p. 216) due to rising greenhouse gas levels. At the same time it cautions that significant natural variability precludes attribution of past drought and flood trends to anthropogenic forcing (p. 233, 240). Some other recent studies (van der Wiel 2016, Bishop et al. 2019, Christy 2019) have likewise noted that mismatches between climate model simulations and observations, as well as the magnitude of natural variability itself, indicate that natural variability is likely the dominant cause of observed historical changes in US precipitation.

Our study aims to provide further evidence about the range of natural variability in some common metrics of US regional precipitation and its relation to the challenge of trend detection. As we will show, it is far from straightforward to say whether rainfall has increased across regions or at a specific location. Adjacent locations may exhibit different trends, trends that emerge over a chosen time span may disappear or even reverse in longer or shorter samples, and trends in one metric may differ from those in another. Deciding whether a trend is statistically significant requires making an assumption about the form of natural variability in the stochastic component of a trend regression model. Unfortunately, the time scale and span of analysis is often dictated by the

availability of data, rather than being determined by the identification requirements of the underlying stochastic process. It has long been known that many hydrological and other climatic processes exhibit long term persistence (LTP), also known as the "Hurst" phenomenon (Mandelbrot and Wallis 1969, Koutsoyiannis 2002 & 2013, Rybski et al. 2006, Varotsos and Efstathiou 2019), which manifests as a slow decay of autocovariances and a clustering tendency over long time spans in which, for instance, wet years tend to follow wet years, slowly giving way to a new cluster in which dry years follow dry years. Trend models with errors that assume independence (ordinary least squares or OLS) or exponentially-decaying autocorrelations (such as one-lag autoregression or AR1) are not suitable under LTP behavior (Koutsoyiannis 2002, Cohn and Lins 2005) because they have a tendency to over-reject the no-trend null; in other words, to over-detect trends.

Two other difficulties in trend detection and attribution have been noted. First, data inhomogeneities may induce spurious trends, especially since measuring methods changed in many locations in the 1970s (Dai et al. 1997, van der Wiel 2016). Second, the sign of trends can vary depending on the start date of the sample, see for example van Wijngaarden and Syed (2015), in which the direction of change in 20th century global precipitation reverses depending on the sample start date. Consequently, reliable detection of an ongoing trend on the century span should be checked not only by examining longer samples, but also checking if the trend magnitude holds up in the closing decades.

In this paper we explore these issues by building and examining long data sets related to precipitation in two US regions, the southeast (SE) and Pacific coast (PC). The first data set is a millennial-span, annual-scale proxy-based reconstruction of the Palmer Modified Drought Index (PMDI) covering calendar years 0—2018. The second consists of observed long-term daily

precipitation records for 20 locations in the SE and PC regions going back at least to 1889, and to 1872 in 11 places. We use the daily records to estimate trends in a variety of metrics of central and extreme annual precipitation: average, median of non-zero days, maximum, variance, downpour occurrence, and 1-day and 2-day 99th percentile exceedances, as well as 2-day extreme 5-year and 50-year return events.

There is a close connection between precipitation changes and drought occurrence, although other weather conditions play a role. Griffin and Anchukaitis (2014) found that while the 2012-2014 California drought was exceptional in the paleoclimate record, the reduction in rainfall was not. The intensity of soil drying arose due to the interaction between an extended lack of rainfall and unusually high temperatures. Ganguli and Ganguly (2016) discuss further that while "meteorological drought" (reduced precipitation) is often a precursor to "hydrological droughts" (deficits in surface and sub-surface water availability) other conditions are needed for the latter to become severe. Consequently, analysis of both types of records is helpful for understanding the full scale of natural variability.

The SE and PC regions were previously examined in Christy (2019), which introduced the first version of the daily precipitation records used here. We have extended the records in some locations, replaced a series from Quitman Georgia (GA) that was difficult to homogenize reliably with a longer and better quality record from Savannah GA, and corrected a number of small errors in the earlier dataset edition. Based on summary analysis, Christy (2019) concluded that mean precipitation had not changed over a 145 year span and on a regional basis there was an indication of increased extreme rainfall in the SE and a decrease in the PC region, but that paper did not undertake statistical modeling to ascertain significance. Like Bishop et al. (2019) in their analysis of

the SE region, Christy (2019) noted that the spatial pattern of change in the PC region did not match that predicted by climate models under GHG forcing, making it likely that natural variability was the dominant cause of observed changes.

A number of studies have examined drought histories in the US Southwest (SW) region. Coats et al. (2014) showed that megadroughts occur regularly in the SW in both paleoclimate reconstructions and in forced and unforced preindustrial climate model runs over the past millennium. Ault et al. (2012) combined paleoclimate and modeling data to argue that the risk of a near-future megadrought in the SW was higher than greenhouse-forced climate model scenarios alone would suggest. We will show that the paleoclimate records from the neighboring PC and SE regions indicate periodic natural tendencies to extended dry (or wet) conditions, echoing the evidence in Coats et al. (2014). Ganguli and Ganguly (2016) studied two decadal-span data sets covering meteorological drought conditions in all US regions, one over the 1926—2013 interval and one over the 1950—2009 interval. They conclude that the spatial extent of extreme meteorological drought in the latter part of the sample exceeds that in the early part, so that areal extent in recent years exceeds that even during the 1930s, although the persistence of extreme meteorological drought has not increased. Evidence for increased drought severity is mixed among regions and between data sets.

Our data sets permit variations in both the time span (sample length) and time scale (data frequency) of analysis. Both types of variation are important. One of the points emphasized in the literature on Hurst phenomena is that change processes that operate on different time scales can lead to complex stochastic properties that only emerge over long time spans. We examine hydrological changes on the millennial, century and decadal time spans. The 2,000-year proxy

series exhibit LTP. Examining daily rainfall records over the 1901-2017 interval to parallel the USGCRP period of analysis, we identify apparently significant upward trends in some average and extreme precipitation metrics in the SE, along with a slight tendency for negative trends in the PC. This matches the general USGCRP findings regarding historical trends, but when we extend the longest series back to 1872 the trends in extreme events largely disappear. Also, they disappear when we confine the sample to the post-1978 portion, even though this is the period with most rapidly rising greenhouse forcing, suggesting that natural mechanisms are likely dominant. We find, overall, that the time span of analysis matters when interpreting changes in US precipitation data. Apparent trends on 117-year data series are not robust either to lengthening or shortening the sample length and may simply be a manifestation of millennial-scale LTP. Our data sets provide evidence that average and extreme US precipitation metrics have not moved outside the bounds of natural variability as best we can measure it.

2 DATA

2.1 PROXY PMDI RECONSTRUCTION

The yearly PMDI precipitation amount is estimated from tree ring characteristics by Cook et al. 2010, and dynamically updated to the current time by Gille et al. https://www.ncdc.noaa.gov/paleo-search/study/22454). The metric calculated is the summer PMDI which because it represents a time-integrated value of hydrologic drought is strongly related to precipitation during the previous several months ($r \sim 0.7$ vs. the precipitation totals here). From the half-degree gridded time series the PC and SE regions were delineated.

Figure 1 shows the PC and SE proxy series after applying a 30-year moving average filter to dampen excursions on time scales shorter than those customarily associated with climate. The series means are arbitrarily chosen to make the display easier to read. The year 1900 is indicated by the vertical dashed line. Both regions clearly exhibit natural variability on relatively long time spans. For example the (filtered) SE proxy values drop from about -0.4 to -2.1 from AD 625 to 725 then reverse upwards to -0.1 by 790. The filtered PC proxy values swing between 1.6 and 0.6 between AD 700 and 1000, then oscillate between 0.7 and 1.3 three times during the interval from 1000 to 1300. A researcher looking only at the post-1900 interval would conclude that the PC region has experienced a reduction in moisture and the SE region has experienced an increase. But extrapolation of such trends into the future would be unwise. The magnitude of changes in the post-1900 interval (PC 0.9, SE 1.0) are within those of the preindustrial-era, indicating that 20th century excursions do not exceed the range of natural variability, which has in the past yielded reversals of direction every few decades.

2.2 Regional Daily Precipitation Records

In our two US climate regions, each has ten stations with continuous daily records beginning by 1889 and with most stations several years prior. All are current through 2018. The locations are as shown in Figure 2, in which the color code indicates the trend in the annual average of daily precipitation in mm/year. Stations in PC are (north to south) in the state of Oregon: Astoria (AST), Portland (PTL), Salem (SLE), and in California: Eureka (EKA), Red Bluff (RBL), Sacramento (SCT), San Francisco City (SFOC), Fresno (FNO), Los Angeles downtown (LOX) and San Diego (SAN). The climate of this region is generally Mediterranean in which the majority of precipitation events occur

early in the winter season, beginning in October and becoming mostly dry by May. Because of this regime, we shall use the water-year (1 Oct to 30 Sep) as the annual time period for the analysis. Thus a year indicated as "2017" for example refers to the water-year 1 Oct 2017 through 30 Sep 2018.

The stations in SE are relatively near the Gulf of Mexico and Atlantic coasts. These sites were selected to avoid snow events as much as possible because of the varying ways in which snowfall and liquid equivalent precipitation were measured throughout the year. These stations reside in a humid, subtropical environment with substantial precipitation possible in any month, but with a minimum in late summer and fall. As such, we shall utilize the water year Oct-Sep as well. The stations (west to east) are Shreveport LA (SHV), Vicksburg MS (VKS), New Orleans LA (NEW), Mobile AL (MOB), Pensacola FL (PEN), Montgomery AL (MGM), Augusta GA (AUG), Jacksonville, FL (JAX), Savannah GA (SAV) and Charleston downtown SC (CHSC).

The data were accessed through various sources in the US; (a) the Global Historical Climate Network Daily files on the Climate Data Online website operated by the National Centers for Environmental Information (NCEI), available online at https://www.ncdc.noaa.gov/cdo-web/search, (b) NCEI's image archive of original paper documents of weather observation forms and monthly reports, available at https://www.ncdc.noaa.gov/IPS/coop/coop.html, (c) the Forts archive operated by the MidWest Regional Climate Center, available at https://mrcc.illinois.edu/data_serv/cdmp/cdmp.jsp, and, (d) xmACIS2 operated by the Northeast Regional Climate Center, available at https://xmacis.rcc-acis.org/. All data were recorded and retrieved in inches to 0.01 precision (one hundredth of an inch) and converted to mm with precision of 0.1 (one tenth mm) for this analysis. In several cases where the digital archives

indicated missing values after 1890, the values were found on the climatological forms and, though manually intensive, were able to be filled by retrieving and examining these forms. The very few missing values were infilled by values observed at nearby stations.

Table 1 indicates the earliest year available for each station (which typically is not the start year of the analyses herein). The variation in start dates allows us to use all stations as of 1889, as well as a subset of 11 stations (5 PC, 6 SE) that have complete records back to 1872. These are indicated by an asterisk. Table 1 lists summary statistics based on the post-1889 sample (mean in mm/day, median of non-zero days in mm/day, variance and maximum) for daily totals for each location. Table S2 in the Supplement lists the same information for 2-day totals (formed as the sum of the daily total and the previous day's). The tables also report the trend in mm/year, the lower- and upper-95 percent confidence interval bounds on the trends, and a significance score for the trend. The last three items will be discussed in the next section.

For each location we also computed the following metrics over the post-1889 interval: annual average; annual median of non-zero days; annual variance, annual maximum, annual occurrences of a downpour (defined as more than 25.4 mm in one day), annual number of times 1-day rainfall exceeded the 99th percentile of 1-day totals in that location and the annual number of times the 2-day rainfall total exceeded the corresponding 99th percentile in that location. Figures 3 through 5 show, for each location (PC top two rows, SE bottom two rows), average annual precipitation, the annual maximum and the annual 2-day 99th percentile exceedances. The annual observation is shown as a light grey circle and the black line is a cubic spline smoother. The remaining graphs and all summary tables are in the Supplement. The graphs not shown appear sufficiently similar to those shown that they are not needed herein.

Consistent with the proxy record, SE locations show a general tendency toward more precipitation and a rising maximum whereas PC locations do not. Looking at the annual averages it is apparent that the PC exhibits more within-region variation than does the SE, both regarding the amounts and the directions of change. Except for Astoria OR, the PC locations tend to have less rain and a lower annual maximum than those in the SE. They also exhibit no tendency towards increased 2 day 99% exceedances, whereas many locations in the SE exhibit a slightly positive trend. Formal statistical inferences will be presented in the next section.

Another commonly-used metric of extreme rainfall is based on the wettest 2-days in each non-overlapping 5-year segment or pentad. There are 25 pentads available in each location from 1893-94 to 2017-18. For each location the 25th-wettest 2-day interval over the entire post-1893 interval was used as a cut-off, and then the number of times this was exceeded per pentad was computed. These counts were then averaged across the PC and SE regions respectively, and the results plotted in Figure 6. If once-every-5-year extreme rainfall events were distributed uniformly across the sample we would observe horizontal lines at 1.0 for both regions. As shown, while there are deviations around that result, there is no tendency towards increasing or decreasing 2 day extreme 5-year return events in either region. The linear trend coefficients (events per pentad) are shown in the graph; neither one is statistically significant.

Since 5-year return events are not of significance for large planning projects we also looked at extreme 50-year return events, defined as follows. There are 75 overlapping 50-year windows ending in years from 1943 to 2017. We identified for each location the 75th-largest 2-day rainfall event, computed the number of days exceeding this count in each moving 50-year window, then averaged this number across regions. If extreme events are independent across time, in a 125 year

sample, every day has a probability of exceeding the cut-off equal to $75 \div (125 \times 365)$. A 50-year window then has a null expectation of containing this number times 50×365 events, which is 30. Figure 7 shows the number of extreme 50-year return events in each 50-year window ending in the years shown from 1943 to 2017 for each region. The pattern is quite different compared to Figure 6. PC exhibits a steady decline from the 1940s until the mid-1990s then levels off. SE exhibits no trend but there is a jump at the end. The trend coefficients (showing the changing number of expected events per year) are both significant. However, in the SE, this is entirely due to the final 3 years (2015-17): if they are removed its trend coefficient becomes 0.004 and is insignificant.

Summarizing our data, the proxy measures and the daily precipitation records both indicate 20th century net drying in the Pacific region and moistening in the Southeast. But the proxy record exhibits variability in long term drought events on the millennial span that match or exceed changes in the 20th century. On daily and annual levels we find evidence of location-specific variability, but no indication of a trend towards increased 2-day extreme 5-year return events in either region. The PC region shows a definite decline in extreme 1-in-50 year 2-day precipitation events; the SE region shows no trend over most of the sample but a large jump occurs in the years 2015-17. We now turn to the formal statistical analysis.

3 STATISTICAL ANALYSIS

3.1 PROXY PMDI RECONSTRUCTION

Figure 8 shows the first 200 lag autocovariances (except the first lag) of the two proxy series. For comparison, the dashed lines show the corresponding autocovariances of a 1-lag autoregressive

(AR1) model with an AR coefficient of 0.9. Even though that would be considered a very "red" series, namely one with strong autocorrelation, it is nonetheless clear that its autocovariances decay exponentially and by about 75 lags they have vanished, yet those of the proxy drought series exhibit no such tendency. This indicates, in an informal way, that the drought series exhibits "long memory" which we will herein characterize using an LTP model.

There are several ways of explaining long memory or LTP, each of which works by introducing a simple time series process whose structure implies autocovariances that decay much more slowly than those of a standard autoregressive process. Koutsoyiannis (2013) provides an insightful survey of the underlying ideas, pointing out that metaphorical terms like "long memory" and persistence are intrinsically unsatisfactory, because the underlying idea is not simply long chains of autocorrelated causation, but ongoing processes of change that exist on multiple overlapping time scales; the persistent autocorrelation pattern is a consequence not a cause of the change structure.

Following Koutsoyiannis (2002) and (2013), consider a time series of independent and identically distributed (iid) observations X_t where t denotes the time index $1, \ldots, N$. Suppose the expected value of X_t is μ and its variance is σ^2. Now replace X_t with $X_t^{(2)}$ where the superscript (2) denotes that the series consists of $N/2$ means of non-overlapping pairs of adjacent values: $(X_1 + X_2)/2, (X_3 + X_4)/2$, etc. Similarly $X_t^{(3)}$ denotes the sequence of $N/3$ non-overlapping means of 3 observations $(X_1 + X_2 + X_3)/3, (X_4 + X_5 + X_6)/3$, and so forth to $X_t^{(k)}$ where the maximum possible value of k is $N/2$ (in practice $k \leq N/10$ is more commonly used). It can be shown that for any k, if X_t is iid, the expected value of $X_t = k\mu$ and its standard deviation is $\sigma k^{-0.5}$. If we vary k and plot $\log(\sigma k^{-0.5})$ it should have a slope of -0.5. A series that exhibits Hurst behavior, however, has a

variance process that accumulates at the rate σk^{H-1} where $0.5 \leq H \leq 1$. In this case the autocovariances do not decay exponentially except at the lower bound.

This characterization works when the series is stationary, specifically if it has a constant and finite variance. Some forms of nonstationarity imply the variance σ^2 goes to infinite, but the variance of increments $(X_{t+\tau} - X_t)$ is finite and constant. For example, if the series consists of evenly spaced annual observations and t denotes the year, the time step $\tau = 1$ implies the annual differences are stationary. If the series is annual and $\tau < 1$, implying increments less than a full year in length need to be taken to yield a stationary series, then the series is said to be "fractionally differenced", and it exhibits some unusual properties, including long memory.

Each long memory model implies a parameter that characterizes the LTP process, and there have been numerous proposed estimation methods. Here we use the smoothed periodogram method of Reisen (1994) which yields a fractional differencing parameter *d* which falls in the region $(-0.5,1.0)$. A value of $-0.5 < d \leq 0$ implies exponential decay of the autocovariances consistent with Ordinary Least Squares (OLS) and general AR models, $0 < d < 0.5$ implies that the series is stationary and mean-reverting but subject to LTP, and $0.5 < d \leq 1.0$ indicates nonstationarity. Hydrological series typically exhibit *d* values in the range of 0.2 to 0.4. In trendless artificial data with $d = 0.3$, OLS and AR1 trend models rejected the no-trend null 25—40% of the time, implying very large type I error rates (Cohn and Lins 2005). Consequently, considerable caution needs to be exercised when inferring trends in century- and decadal-length data when LTP is present.

The ratio of d to its standard error is asymptotically standard normal under the null hypothesis of $d = 0$. In our proxy sample the estimates[1] of d are 0.29 and 0.10 for the PC and SE regions, respectively, with corresponding ratio values 6.7 and 2.1, indicating the presence of long memory in the long-term regional proxies.

3.2 Daily Precipitation Records

3.2.1 LTP Analysis

LTP is not reliably detected in the modern records. In the daily data, the d parameters and corresponding ratios over standard errors for the post-1889 PC and SE regional averages are, respectively, -0.02 (-1.32) and 0.06 (3.78), indicating no LTP in the Pacific daily records and a small but significant LTP process in the SE. But in the annual averages while the d parameters are larger in magnitude and similarly opposite in sign, they are respectively -0.27 (PC, ratio -2.20) and 0.13 (SE, ratio 1.09). The instability of the d values and the fact that when positive they are not significant indicates that trend analysis on annual records based on the assumption of short memory is likely valid, subject to the caution that the standard errors likely exhibit complex autocorrelation patterns. "Validity" here refers to the sample characteristics: the inability to detect LTP arises because the sample time span is inadequate to identify long range correlations.

[1] We estimated d using the fdSperio routine in the R statistical package.

Iliopoulou et al. (2018) also found evidence of LTP in long proxy records but only weak evidence in annual instrumental precipitation records. They cautioned that the instrumental sample length may be inadequate to identify long-range dependence. This point was also made in Markonis and Koutsoyiannis (2016) who showed that instrumental records spanning about 100 or 200 years did not clearly reveal LTP found in collocated proxy records of much longer sample length (2400 years), and likewise short segments of long proxy records individually look like white noise even though the series as a whole exhibits LTP. Although we are using very long records of daily rainfall, the same limitation may be at issue here.

3.2.2 Trend Analysis

We use OLS to estimate linear trend coefficients. Computing unbiased variances is a challenge when the data are autocorrelated. A common approach is to fit an AR model, but it has become more popular in time series analysis in recent decades to use non-parametric methods. These are usually based on functions of the OLS residuals that can be shown theoretically to yield consistent coefficient matrix estimators regardless of the underlying form of autocorrelation.[2] We use the method of Vogelsang and Franses (2005, denoted VF) to compute confidence intervals and trend significance tests. The VF method is robust to general forms of autocorrelation although not LTP. If the true process is AR1 the VF estimator performs similarly to it in the sense that it yields very similar 95 percent confidence intervals, but unlike a parametric AR1 model it remains valid if the

[2] "Consistent" is used herein in its statistical sense of a probability limit converging to an unbiased point estimate.

lag length of autocorrelation increases. The trend coefficients for the 1889-2017 interval are as shown in Figure 1. Confidence intervals and test scores are reported in the last three columns of Table 1 based on the VF method. The 95% critical value of the VF test score is 41.53, indicating that only Charleston, Mobile, Pensacola and Shreveport exhibit significant positive trends in daily precipitation totals, with Vicksburg marginally significant. Astoria has a negative and significant trend.

The regional trend analysis on annual metrics are summarized in Table 2. Here the trend coefficients are computed on the regionally-averaged series in order to correspond to the regionally-averaged PMDI proxy indicator. Numerical trend values and statistics for individual locations and regional groupings are available in the Supplement. The coding for Table 2 is as follows: − negative and significant, (0) negative and insignificant, 0 positive and insignificant, + positive and significant. Beginning with the first block, we examine the 1901—2017 interval to match the time period of analysis in USGCRP (2017). The first three columns measure trends in the center and spread of the distribution while the last four measure trends in extreme metrics. The PC results are uniformly negative and insignificant. In contrast the SE trends in the annual mean and median and the various metrics of extreme precipitation are positive and significant except for the annual maximum. If we confined our analysis to this time span and this level of averaging we would conclude that average precipitation in the US Southeast has risen, as shown in a variety of measures of central and extreme precipitation, and taking the combined 20-location average as a whole (third row) we would draw similar conclusions for the entire continental region covered by our sample. This, in turn, might seem to offer supporting evidence of the hypothesis that rising greenhouse

gases levels will lead to more precipitation on average and a greater tendency for extreme weather events.

However our analysis thus far shows that caution is warranted when a single time interval is being analysed. The next block reports results using the subset of locations with longer records. Note that, using this subset but keeping the start date at 1901 we get almost identical results as in the top block of Table 2 (the Combined annual average trend becomes significant, the Pacific median trend becomes insignificant and the SouthEast maximum trend becomes insignificant; other results remain the same). But upon including the additional years back to 1872, the results become as shown in the middle block. Positive trends in the SE median and maximum are offset by negative trends in PC, and other than that the regional trends are almost all insignificant, and the regionally-combined trends all become insignificant.

The proxy records indicate that trend reversals can occur on sub-century sample lengths. The third block in Table 2 shows results using the annual data from 1978 to 2017, comprising the final 40 years of the data and potentially avoiding possible spurious trends due to equipment changes in the 1970s. Many signs change, and all significant trends in the extreme metrics disappear. If rising GHG forcing were the dominant factor in the post-1901 data we would not expect these trends to reverse or weaken, since this is the segment when GHGs rise most quickly.

Not shown in the tables is a set of regressions just on fall precipitation since 1958. This sample cannot start later than 1958 since San Francisco had no downpours thereafter, making the variance matrix non-singular. Every entry in a block corresponding to the format of Table 2 is 0 or (0), indicating no trends in average or extreme fall precipitation in either the SE or PC regions over the past 60 years.

Summing up, while trends can be identified on some time spans, on the longest samples the trends are not significant, nor are they significant over the shorter interval of enhanced greenhouse forcing, and the proxy data exhibit long term persistence. Taken together these findings are consistent with the view that natural variability is likely the dominant factor in historical US precipitation changes through to the present time.

4 DISCUSSION AND CONCLUSIONS

In their studies of various US regions, Van der Wiel et al. (2016), Christy (2019) and Bishop et al. (2019) all concluded that to the extent GHG forcing is adding a trend to observed precipitation rates it remains small relative to natural variability. Our findings support this, and point to the need to be careful when trying to identify a trend which is to be attributed to either cause. Application of standard trend estimation methods in data sets that exhibit long memory or LTP can cause spurious trend detection (Cohn and Lins 2005). The issue is visible in Figure 2: selection of any century-scale subset could easily lead to an erroneous conclusion that a significant trend has been identified, even though the series as a whole is not trending. Trend extrapolation even when qualitatively supported by a hypothesis about the influence of rising GHG levels would be perilous given the natural tendency for persistent mean reversions.

We explore these issues by varying the time span of analysis and using statistical methods appropriate to the error processes. In a sample of daily precipitation records that extend back to the late 1800s if we confine attention to the post-1901 interval we generally replicate the USGCRP (2017) findings of significantly increased SE moisture and rising occurrences of some extreme

precipitation metrics. But these trends are not robust to extending the start date of the data set back to 1872, and they disappear in the post-1978 interval of the data, even though it is the interval during which GHG forcing sharply increased. Thus natural variability is likely the dominant driver of historical changes in precipitation in the regions covered by our analysis.

5 REFERENCES

Ault, T.R., Cole, J.E., Overpeck, J.T., Pederson, G.T., Meko, D.M. (2014) Assessing the Risk of Persistent Drought Using Climate Model Simulations and Paleoclimate Data. *Journal of Climate* 27, 7529-7549. https://doi.org/10.1175/JCLI-D-12-00282.1

Bishop, Daniel A., A. Park Williams, Richard Seager, Arlene M. Fiore, Benjamin I. Cook, Justin S. Mankin, Deepti Singh, Jason E. Smerdon, and Mukund P. Rao (2019) Investigating the Causes of Increased Twentieth-Century Fall Precipitation over the Southeastern United States. *Journal of Climate* Volume 32 December 2018, https://doi.org/10.1175/JCLI-D-18-0244.1

Christy, J.R., (2019) Examination of extreme rainfall events in two regions of the United States since the 19th century. *AIMS Environmental Science,* 6(2): 109–126 DOI:10.3934/environsci.2019.2.109.

Coats, Sloan, Jason E. Smerdon, Benjamin I. Cook and Richard Seager (2015) Are Simulated Megadroughts in the North American Southwest Forced? *Journal of Climate* January 2015 https://doi.org/10.1175/JCLI-D-14-00071.1

Cohn, Timothy A. and Harry F. Lins (2005) Nature's Style: Naturally Trendy. *Geophysical Research Letters* 32, https://doi.org/10.1029/2005GL024476.

Cook, E.R., Seager, R., Heim, R.R., Vose, R.S., Herweijer, C., and Woodhouse, C. (2010). Megadroughts in North America: Placing IPCC projections of hydroclimatic change in a long-term paleoclimate context. *Journal of Quaternary Science*., 25(1), 48-61. doi: 10.1002/jqs.1303

Dai, Aguo, Inex Y. Fung and Anthony D. Del Genio (1997) Surface Observed Global Land Precipitation Variations during 1900–88. *Journal of Climate* 10 November 1997 https://doi.org/10.1175/1520-0442(1997)010%3C2943:SOGLPV%3E2.0.CO;2

Ganguli, P. and Ganguly, A.R., (2016) Space-time trends in U.S. meteorological droughts. *Journal of Hydrology: Regional Studies* 8, 235-259 https://doi.org/10.1016/j.ejrh.2016.09.004

Griffin, D. and Anchukaitis, K.J., (2014) How unusual is the 2012-2014 California drought? *Geophysical Research Letters* 41, 9017-9023 https://doi.org/10.1002/2014GL062433

Iliopoulou, T, S.M. Papalexiou, Y. Markonis, and D. Koutsoyiannis (2018) Revisiting long-range dependence in annual precipitation, *Journal of Hydrology*, 556, 891–900, doi:10.1016/j.jhydrol.2016.04.015.

Koutsoyiannis, Demetris (2002) The Hurst Phenomenon and Fractional Gaussian Noise Made Easy. *Hydrological Sciences Journal* 47(4) https://doi.org/10.1080/02626660209492961

Koutsoyiannis, D (2013) Hydrology and Change, *Hydrological Sciences Journal*, 58 (6), 1177–1197, doi:10.1080/02626667.2013.804626.

Markonis, Yannis and Demetris Koutsoyiannis, (2016) Scale-dependence of persistence in precipitation records. *Nature Climate Change* 6, 399-401.

Mandelbrot , Benoit and James R. Wallis (1969) Some Long-run Properties of Geophysical Records. *Water Resources Research* Volume 5(2) April 1969 https://doi.org/10.1029/WR005i002p00321.

Reisen, Valderio (1994) Estimation of the Fractional Difference Parameter in the ARIMA(*p*,*d*,*q*) Model using the Smoothed Periodogram. *Journal of Time Series Analysis* 15(3) https://doi.org/10.1111/j.1467-9892.1994.tb00198.x.

Rybski, Diego, Armin Bunde, Shlomo Havlin and Hans von Storch (2006) Long-term Persistence in Climate and the Detection Problem *Geophysical Research Letters* 33(6) https://doi.org/10.1029/2005GL025591

USGCRP, 2017: *Climate Science Special Report: Fourth National Climate Assessment, Volume I* Wuebbles, D.J., D.W. Fahey, K.A. Hibbard, D.J. Dokken, B.C. Stewart, and T.K. Maycock (eds.). U.S. Global Change Research Program, Washington, DC, USA, 470 pp., doi: 10.7930/J0J964J6.

van der Wiel, Karin, Sarah B. Kapnick, Gabriel A. Vecchi,, William F Cooke, Thomas L. Delworth, Liwei Jia, Hiroyuki Murakami, Seth Underwood, and Fanrong Zeng (2016) The Resolution Dependence of Contiguous U.S. Precipitation Extremes in Response to CO2 Forcing. *Journal of Climate* Volume 29 October 2016, https://doi.org/10.1175/JCLI-D-16-0307.1.

Van Wijngaarden, W.A. and A. Syed (2015) Changes in Annual Precipitation over the Earth's Land Mass Excluding Antartica from the 18th Century to 2013. *Journal of Hydrology* 531 http://dx.doi.org/10.1016/j.jhydrol.2015.11.006 0022-1694.

Varotsos, C.A. and M.N. Efstathiou (2019) Has Global Warming Already Arrived? *Journal of Atmospheric and Solar-Terrestrial Physics* 182 https://doi.org/10.1016/j.jastp.2018.10.020.

Vogelsang, T.J. and Franses, P. H. (2005) Testing for Common Deterministic Trend Slopes, *Journal of Econometrics* 126 https://doi.org/10.1016/j.jeconom.2004.02.004.

FIGURES

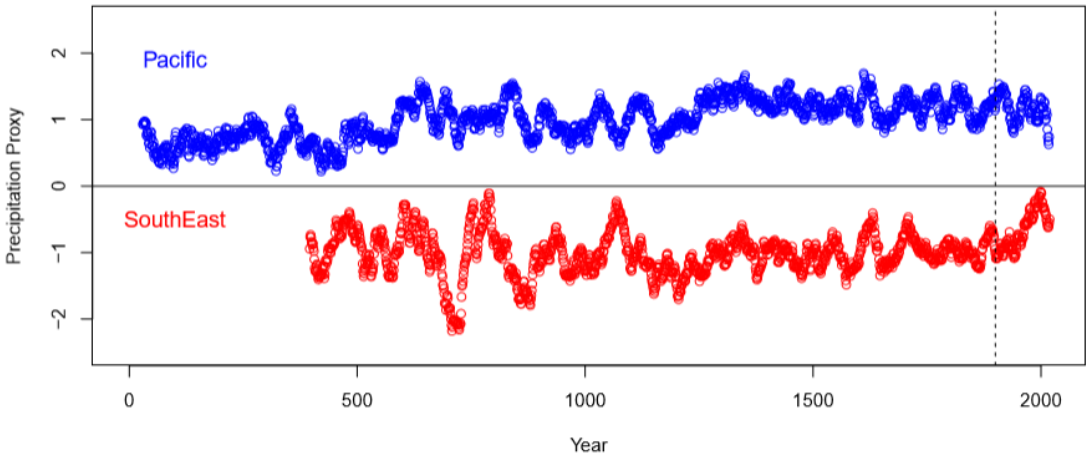

Figure 1. PC and SE proxies for the Palmer Modified Drought Index, filtered using a 30-year moving average. The vertical dashed line shows the year 1900. The series are arbitrarily centered on means of -1 and +1 to aid comparison

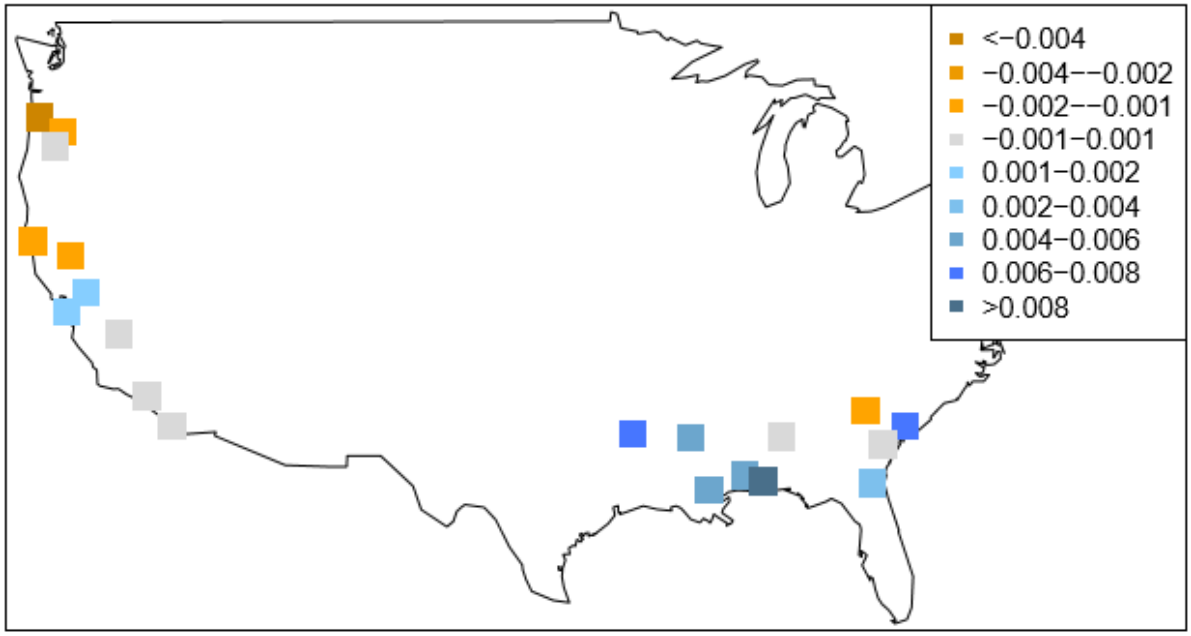

Figure 2. Locations of cities in sample, color-coded by trend in annual daily average (in mm/year) over period 1889—2017.

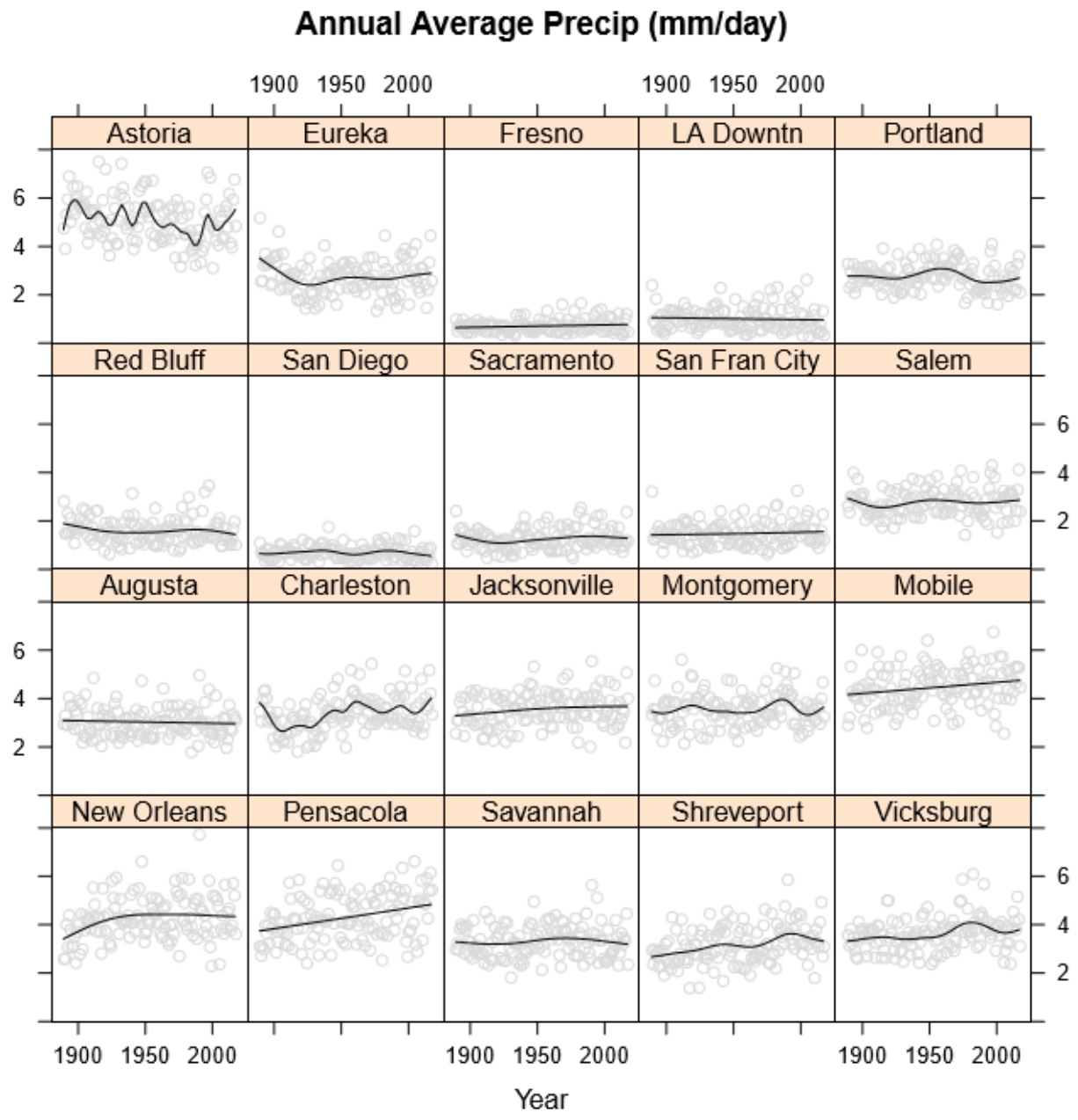

Figure 3: Average annual precipitation (mm/day) 1889-2017 in each of the studied locations with spline smoother shown.

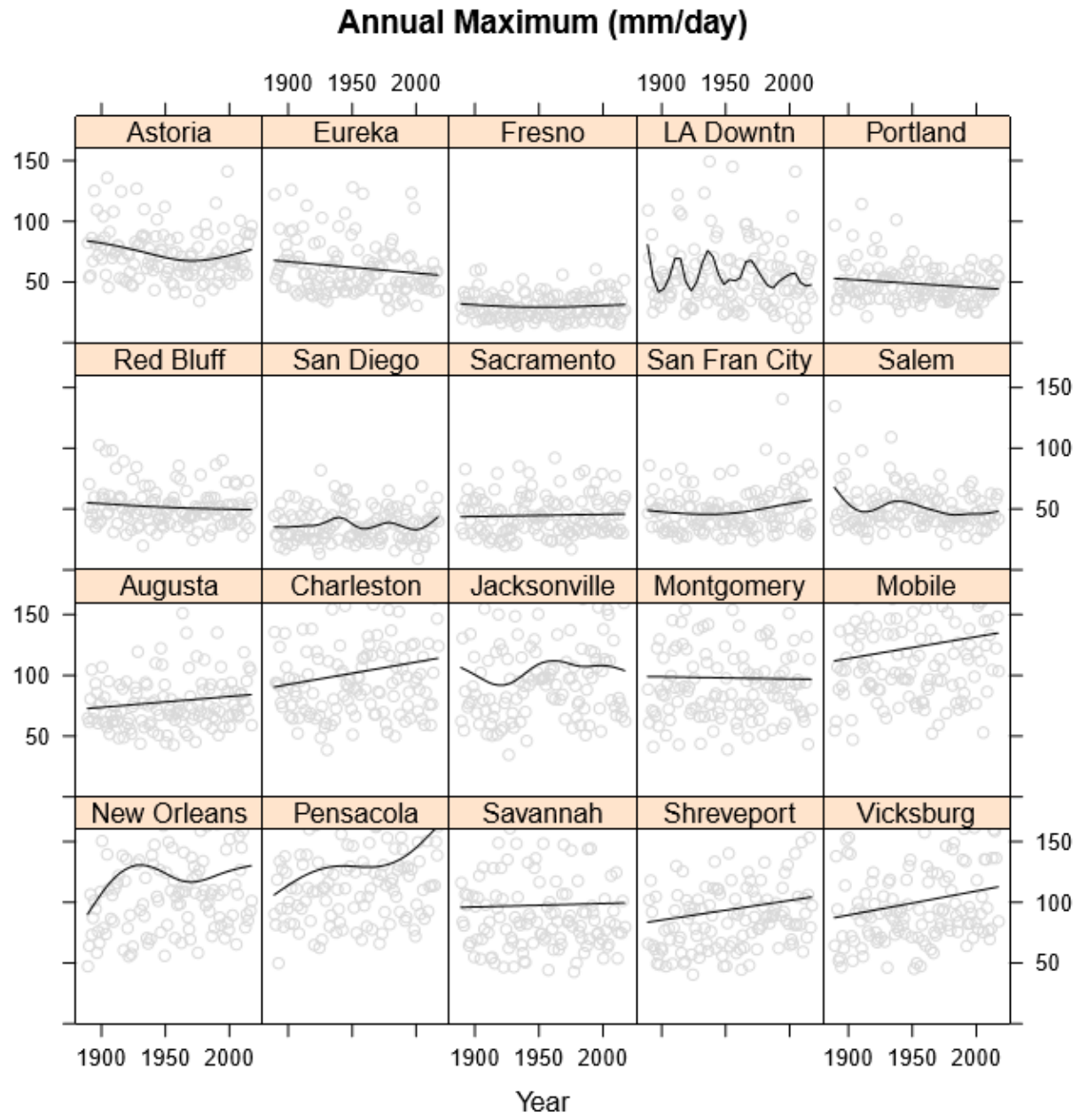

Figure 4: Annual 1-day Maximum Precipitation (mm/day) 1889-2017 in each of the studied locations with spline smoother shown.

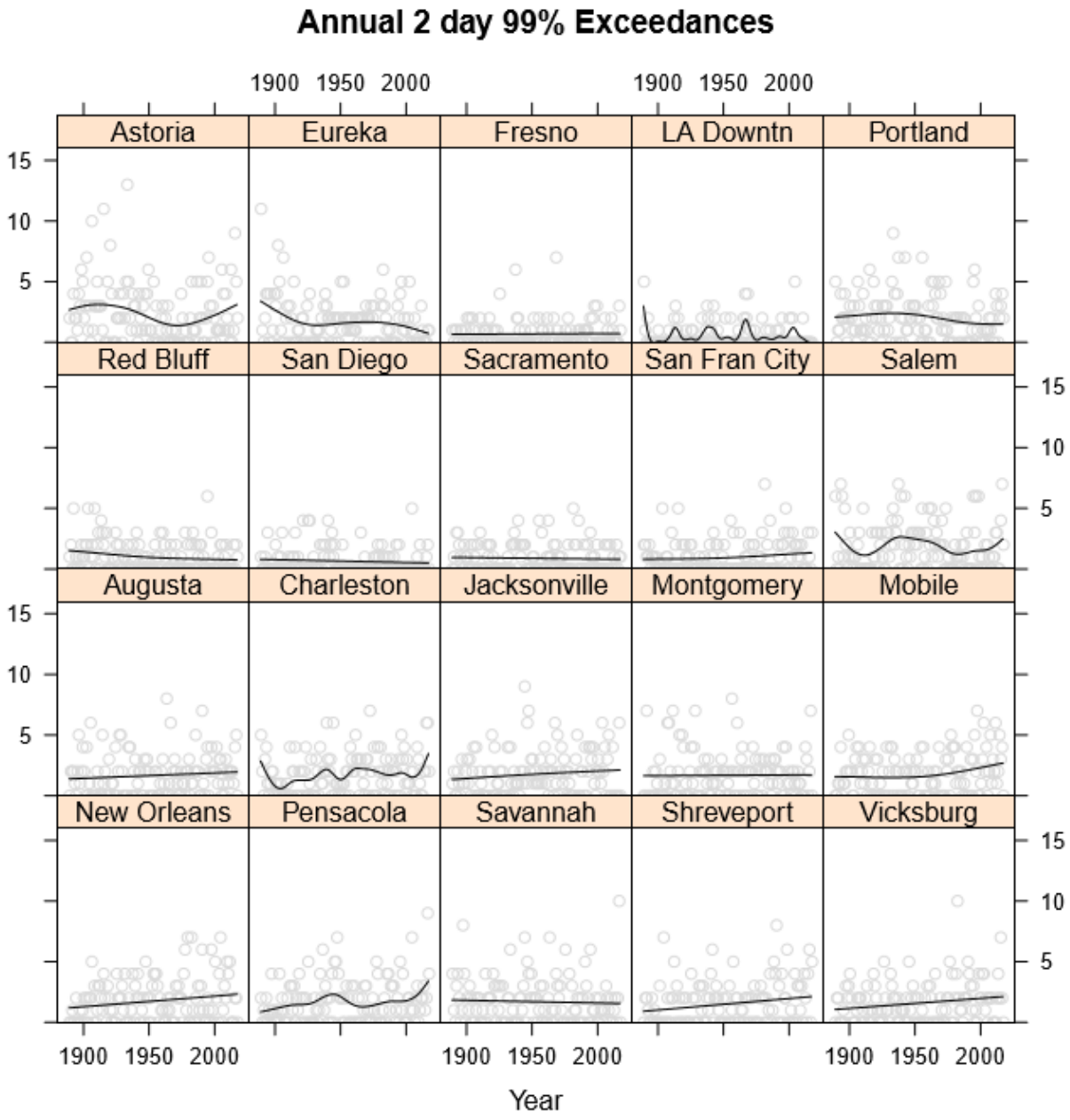

Figure 5: Annual 2-day exceedances of 1889—2017 99th percentile cut-off in each of the studied locations with spline smoother shown.

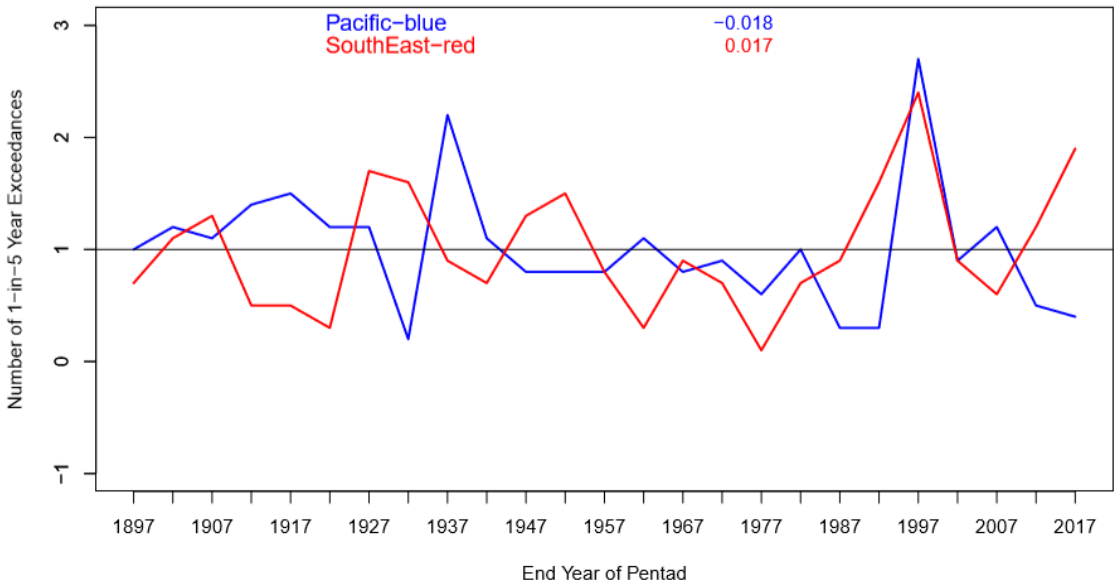

Figure 6: Occurrences of 2-day 5-year return events in each 5-year interval beginning with 1892-1897, averaged by region. Pentads are denoted by the ending year. Numbers shown at top are linear slope coefficients (events per pentad).

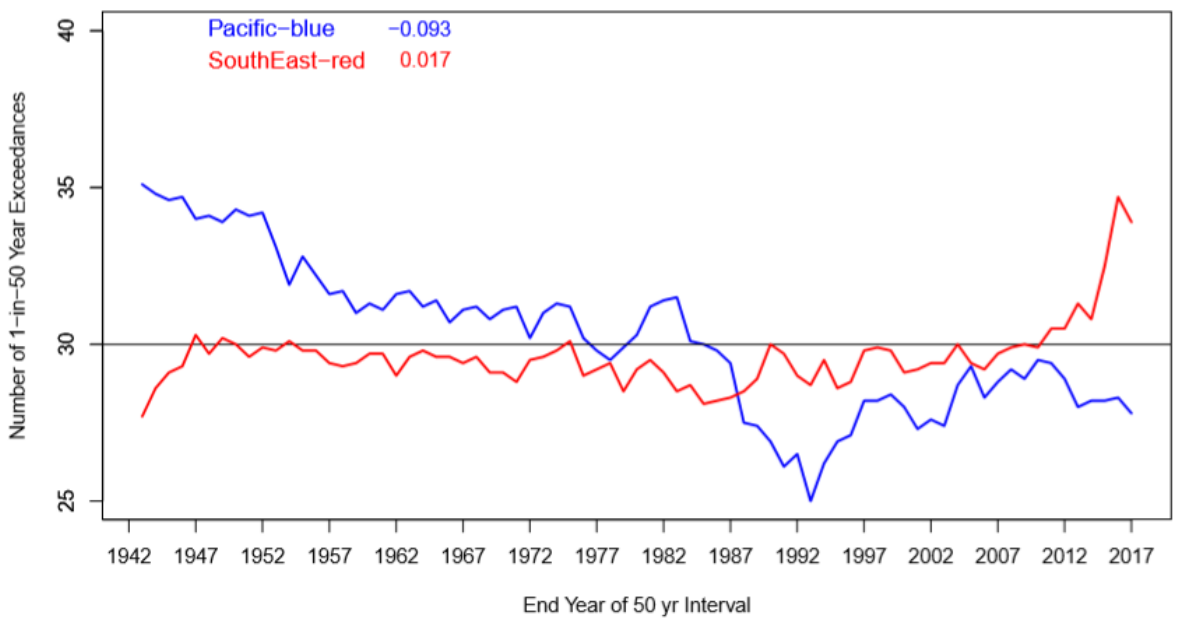

Figure 7: Occurrences of 2-day 50-year return events in each overlapping 50-year interval ending in the year indicated, averaged by region. Numbers shown at top are linear trend coefficients (change per year).

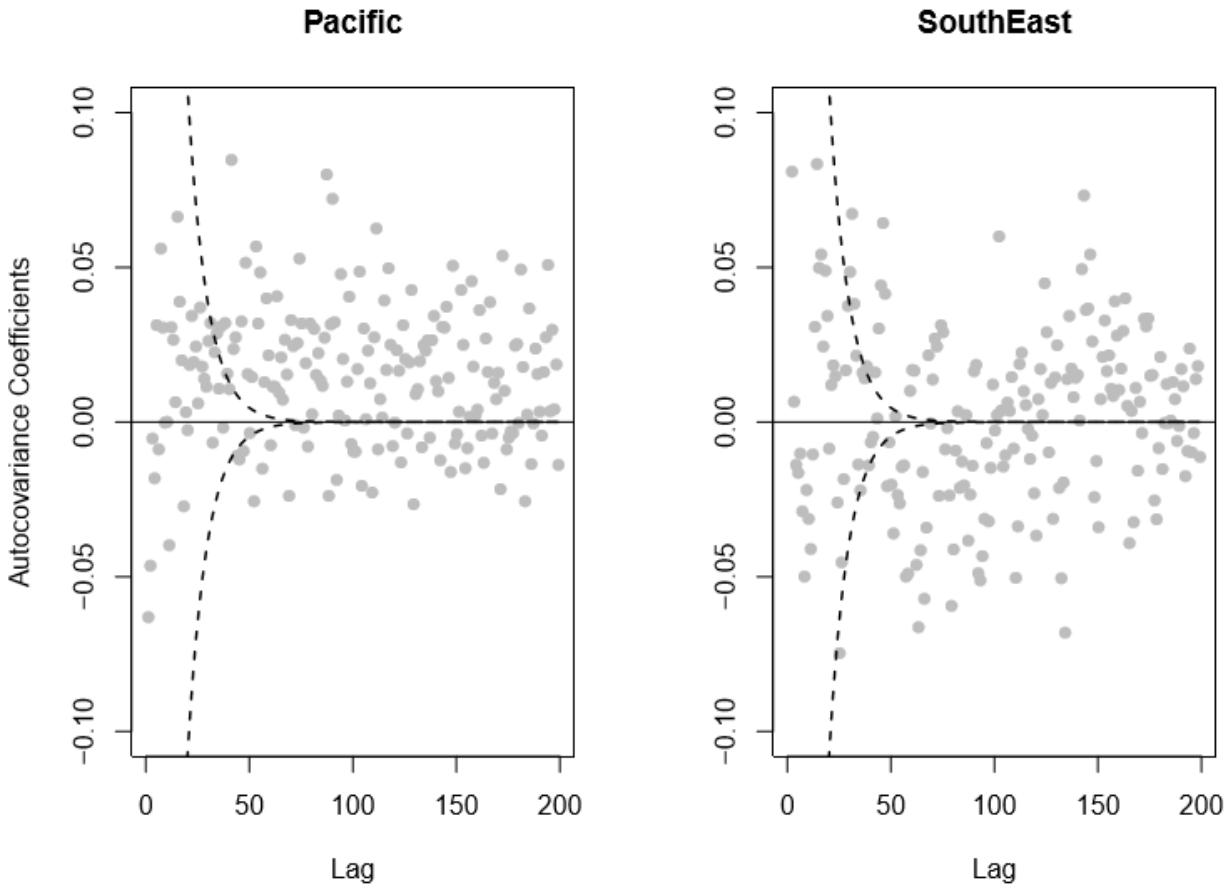

Figure 8: Autocovariance coefficients for lags 2—200 for 2,000-year proxy series from Pacific and SouthEast regions. The dashed lines show, for comparison, the corresponding autocovariances for an AR1 process with lag coefficient of 0.9.

TABLES

1889 – 2017 Daily (mm)

	Earliest Year	Mean	Median	Variance	Max	Trend	CI-lower	CI-upper	VF Score
Astoria*	1871	5.1	5.6	99.2	177.3	-0.007	-0.013	-0.001	53.6
Eureka	1887	2.7	4.1	54.8	172.5	-0.002	-0.010	0.006	1.6
Fresno	1877	0.7	3.3	9.8	60.5	0.001	-0.000	0.002	25.2
LA Downtn	1878	1.0	4.8	29.9	149.4	-0.001	-0.003	0.002	5.5
Portland*	1872	2.8	3.8	38.4	114.3	-0.002	-0.008	0.004	3.3
Red Bluff	1878	1.6	4.1	33.1	102.6	-0.002	-0.006	0.002	6.5
San Diego*	1871	0.7	2.5	12.2	82.0	0.000	-0.002	0.002	1.0
Sacramento	1878	1.3	4.1	23.4	92.2	0.001	-0.002	0.005	5.5
San Fran City*	1849	1.5	4.1	29.3	140.7	0.001	-0.002	0.004	4.2
Salem*	1870	2.8	4.1	41.2	134.6	0.001	-0.003	0.004	1.8
Augusta*	1869	3.0	4.8	79.9	247.9	-0.001	-0.004	0.002	4.1
Charleston*	1872	3.4	4.8	109.8	292.1	0.007	0.000	0.013	47.1
Jacksonville*	1867	3.6	4.8	118.1	249.4	0.003	-0.001	0.008	24.0
Montgomery	1873	3.6	5.6	112.7	246.4	0.001	-0.003	0.005	1.8
Mobile*	1870	4.5	6.1	178.3	339.3	0.005	0.001	0.008	78.8

New Orleans*	1870	4.2	5.8	164.3	355.9	0.006	-0.003	0.014	18.6
Pensacola	1880	4.3	6.1	187.3	395.0	0.009	0.004	0.014	123.0
Savannah	1874	3.3	4.8	105.0	229.1	0.001	-0.003	0.006	3.2
Shreveport*	1872	3.2	5.3	105.0	306.1	0.007	0.003	0.010	149.9
Vicksburg	1889	3.6	6.4	121.9	222.3	0.005	-0.000	0.009	40.0

Table 1: Summary statistics for 20 precipitation locations. 1st 10 entries: Pacific Coast region (PC). Last 10 entries: SouthEast (SE) region. *-denotes part of subsample available at least back to 1872. The trend terms are in mm/year. The VF score refers to the test of trend significance due to Vogelsang and Franses (2005). It has a 5% critical value of 41.53.

Region	Average	Non-0 Median	Variance	Maximum	Downpour Counts	1-day 99% Exceedance	2-day 99% Exceedance
				Time span: 1901 – 2017			
Pacific	(0)	(0)	(0)	(0)	(0)	(0)	(0)
SouthEast	+	+	+	0	+	+	+
Combined	+	0	+	0	+	0	0
				Time span: 1872 – 2017			
Pacific	(0)	−	−	(0)	(0)	(0)	−
SouthEast	0	+	0	+	0	0	0
Combined	0	0	0	0	0	0	(0)
				Time span: 1978 – 2017			
Pacific	0	−	0	0	0	0	0
SouthEast	(0)	(0)	0	0	(0)	(0)	0
Combined	(0)	−	0	0	(0)	0	0

Table 2: Summary of trend analysis results on annual metrics, grouped by region. Codes: − negative and significant, (0) negative and insignificant, 0 positive and insignificant, + positive and significant.